Acta Cryst. (1996). D**52**, 534–542

Structure of the Fab Fragment of SDZ CHI621: a Chimeric Antibody Against CD25

VINCENT MIKOL†

Preclinical Research, Sandoz Pharma AG, CH-4002 Basel, Switzerland

(Received 27 September 1995; accepted 15 January 1996)

Abstract

A specific drug targeted to the IL-2 receptor on activated T lymphocytes could limit acute immunological rejection during organ transplantation. A high-affinity monoclonal antibody directed against the α-chain of the IL-2 receptor (CD25) was chimerized with the constant regions of the human IgG1 heavy and κ light chain resulting in SDZ CHII621 [Amlot, Rawlings, Fernando, Griffin, Heinrich, Schreier, Castaigne, Moore & Sweny (1995). *Transplantation*, **60**, 748–756]. The Fab fragment of SDZ CHI621 has been purified and crystallized ($P2_1$, $a = 39.58$, $b = 59.76$, $c = 102.09$ Å, $\beta = 99.98°$). Its structure has been determined by molecular replacement and refined at 2.6 Å to a crystallographic R factor of 19.7%. The protein exhibits the typical immunoglobulin fold. The complementary determining regions (CDR's) 1 and 2 of both heavy and light chains show similar conformations to other known reported structures whereas the CDR3 from the light chain seems to adopt a novel type of conformation. There is a network of interactions which maintain the CDR3 of both chains together and limit their solvent accessibility. The interaction between V_L and C_L has been strengthened by the chimerization whereas that between V_H and C_H1 has been weakened.

1. Introduction

The use of cyclosporin A in immunosuppressive therapy has greatly improved the outcome in renal transplantation. However, acute immunological rejection is still primarily responsible for deterioration or complete loss of allograft function and nearly 20% of first cadaver renal allografts are rejected (Tilney *et al.*, 1984). This has prompted the search for novel therapeutic strategies which could target those lymphocytes which are specifically alloreactive against the foreign graft without affecting physiological host immune surveillance and normal defense mechanisms. Monoclonal antibodies (mAb's) directed against the IL-2 receptor which is only expressed on the surface of activated T-cells and not in resting or memory T-cells could fulfill the conditions for more specific immunosuppressive agents (Kupiec-Weglinski, Diamantstein & Tilney, 1988). The IL-2 receptor is composed of three subunits: a 55 kDa polypeptide (α-chain, Tac antigen, CD25), a 75 kDa polypeptide (β-chain) and a γ-chain. The IL-2 binding characteristics of the α and β subunits, expressed alone, show a low (10^{-8} M) and intermediate (10^{-9} M) affinity for their natural ligand and the association of the three subunits create a high-affinity receptor (10^{-11} M).

A murine anti-CD25 mAb, RFT5, was selected on the basis of high-affinity binding to the CD25 antigen, estimated at 0.1 nM, and potent inhibition of IL-2 mediated proliferation (Amlot *et al.*, 1995). RFT5 was chimerized with the constant regions of the human IgG1 heavy and κ light chain to prevent human anti-mouse antibody response in patients. This chimeric antibody (SDZ CHI621) has been evaluated in a phase I/II clinical study in human renal cadaver transplantation and has shown very promising results (Amlot *et al.*, 1995). In this paper we report the crystal structure of the Fab (antigen-binding) fragment of SDZ CHI621 determined at 2.6 Å resolution and compare it with other known Fab structures.

2. Materials and methods

2.1. *Notations*

A sequential notation for the residues is employed for SDZ CHI621 and the corresponding numbering scheme of Kabat *et al.* (1991) is given in Table 1. Residues from the light and heavy chains will be denoted with the prefixes L_ and H_, respectively.

2.2. *Protein preparation*

The Fab fragment of SDZ CHI621 was prepared by papain digestion of the antibody at 5 mg ml^{-1} in 100 mM sodium acetate (pH 5.5), 25 mM L-cysteine, 1 mM EDTA (ratio of papain/antibody: 1/100). After 3 h incubation at 310 K, papain was inactivated by adding iodoacetamide to a final concentration of 25 mM. The digest was left in the dark for 30 min and then dialyzed against 100 mM phosphate buffer (pH 8.1) and loaded on a protein-A column. The Fab fragment eluted in the flow through and was separated from the Fc which was eluted with 100 mM citrate (pH 3.0). The Fab fragment was further purified by cation-exchange chromatog-

† Present address: Department of Molecular Modeling and Crystallography, CRVA, Rhône-Poulenc Rorer, 13, Quai J. Guesde, BP 14, F-94403 Vitry/Seine, France. E-mail: mikol@rp.fr.

Table 1. *A conversion table for the SDZ CHI621 sequential and Kabat et al. (1991) numbering systems (FR designates a framework region)*

Kabat *et al.*	Sequential	Region
(*a*) Heavy chain		
3–30	1–28	FR1
31–35	29–33	CDR1
36–49	34–47	FR2
50–52	48–50	CDR2
52A	51	CDR2
53–65	52–64	CDR2
66–82	65–81	FR3
82A	82	FR3
82B	83	FR3
82C	84	FR3
83–94	85–96	FR3
95–102	97–104	CDR3
103–212	105–214	FR4+C_H1
(*b*) Light chain		
1–23	1–23	FR1
24–30	24–30	CDR1
31	—	
32–34	31–33	CDR1
35–49	34–48	FR2
50–56	49–55	CDR2
57–88	56–87	FR2
88–94	88–93	CDR3
95–96	—	
97	94	CDR3
98–214	95–211	FR4+C_L

raphy on a S-sepharose fast flow by a linear gradient 0–1.0 *M* NaCl (20 m*M* MES pH 6.0). The profile of elution shows two peaks. The main one (2nd) was additionally purified by preparative chromatofocusing on a mono P Pharmacia column using a pH gradient from 11.0 to 8.0 (starting buffer: 25 m*M* triethylamine–HCl pH 11.0, eluting buffer Pharmacia Polybuffer PB96 1:10 pH 8.0). The main peak eluting at a pH of 10.5 was recovered, loaded on a gel-filtration column to remove the ampholytes, and concentrated with an Amicon concentrator to 30 mg ml^{-1} in 0.02%(*w/v*) NaN_3.

2.3. *Preparation of the crystals and data collection*

Crystals of the SDZ CHI621 Fab were grown by the hanging-drop method in Corning 24-well tissue-culture plates at room temperature. Crystals could be grown with sodium phosphate, ammonium sulfate and polyethylene glycol (PEG) as precipitant and within the pH range 6–9.0. However, the best and largest crystals were grown out of PEG8000 solution at pH 8.0 with Tris–HCl as a buffer. They reach a size of 2.0 × 0.6 × 0.2 mm within a week (see Table 2).

The X-ray intensity data were collected on a FAST television area detector diffractometer. The X-ray source was a rotating-anode generator (FR571) operating at 40 kV and 80 mA. The evaluation of the measured

Table 2. *Crystal and diffraction data*

Crystal parameters	
Initial drop composition	6 µl, 50 m*M* Tris–HCl pH = 8.0, 7.5%(*w/v*) PEG8000, 0.02%(*w/v*) NaN_3, [SDZ CHI621] = 0.33 m*M*
Well composition	1 ml, 100 m*M* Tris–HCl pH = 8.0, 15.0%(*w/v*) PEG8000, 0.04%(*w/v*) NaN_3,
Crystal size (mm)	2.0 × 0.6 × 0.2
Space group, cell dimensions (Å,°)	$P2_1$, $a = 39.58$, $b = 59.76$, $c = 102.09$, $\alpha = \gamma = 90.0$, $\beta = 99.98$
Number of protein molecule per asymmetric unit, solvent fraction (%), V_M (Å^3 Da^{-1})	1, 54.0, 2.58
Diffraction data	
Number of crystals used, measured reflections, unique reflections	1, 32477, 14331 up to 2.46 Å
R_{sym}(%), independent reflections, resolution (Å)	R_{sym} = 5.7 for 11326 independent reflections up to 2.46 Å
Completeness (%)	90.6 up to 2.6 Å

X-ray intensities was performed by the program *MADNES* (Messerschmidt & Pflugrath, 1987). The crystal has one molecule per asymmetric unit and is monoclinic. Data reduction was carried out with the *CCP*4 package (Collaborative Computational Project, Number 4, 1994). The crystal parameters and diffraction data are given in Table 2.

2.4. *Structure solution and crystallographic refinement*

The structure of the SDZ CHI621 Fab was determined by molecular replacement. The search model included the Fab portion of the HyHel-5-structure (Sheriff *et al.*, 1987) deprived of the CDR's, except the second CDR of the light chain which was conserved because the sequence was identical in both Fab's. The direct-space Patterson search method was employed for rotation searches with the HyHel-5 search model against the SDZ CHI621 Fab data as implemented in *X-PLOR* (Brünger, 1992). A clear solution (12.03σ, 2nd peak: 10.83σ) was produced by the rotation search for data between 8.0 and 4.0 Å which was subsequently refined by a Patterson-correlation procedure and rigid-body refinement. After the Patterson-correlation refinement of the orientations and positions of the four domains of the Fab (V_L, V_H, C_L, C_H1),* the correlation coefficients of the first and second peak were 0.263 and 0.114, respectively. The translation search was then performed by optimizing the standard linear correlation coefficient between the normalized observed structure factor (E_{obs}) and the normalized calculated structure

* V_L is the variable domain, light chain (residues 1–105); V_H is the variable domain, heavy chain (residues 1–115); C_L is the constant domain, light chain (residues 106–210); C_H1 is the constant domain, heavy chain (residues 116–215).

factors (E_{calc}). The position of the model computed by the translation search was $x = 0.22$ $y = 0.5$ $z = 0.22$ in fractional units, giving an excellent packing of the symmetry-related molecules and an R factor of 44.5% between 8.0 and 3.5 Å. Rigid-body R-factor refinement was carried out by running 40 steps of conjugate-gradient minimization with the overall orientation and position of the HyHel-5 search model, followed by 50 steps with the orientations and positions of the four domains of the Fab (V_L, V_H, C_L, C_H1) for data between 8.0 and 3.5 Å. The R factor dropped to 41.9% for data between 8.0 and 3.5 Å. This model was used as a starting point for a round of simulated annealing for data between 8.0 and 2.6 Å (120 steps of C^α-restrained conjugate-gradient minimization, molecular dynamics starting at 3000 K and ending at 300 K over a period of 2.7 ps, followed by 120 steps of conjugate-gradient minimization). After this round of simulated-annealing refinement, the R factor for data between 8.0 and 2.6 Å dropped to 28.8% with r.m.s. deviations of bond lengths and bond angles from ideality of 0.022 Å and 4.4°, respectively. Then $(2|F_{obs}| - |F_{cal}|)\exp(i\varphi_{cal})$ difference maps were computed, side chains were substituted, inserted, or deleted according to the sequence of SDZ CHI621 using the program *O* on an ESV graphics workstation (Jones, Zou, Cowan & Kjeldgaard, 1991). Then alternate rounds of model building followed by least-squares refinement using the program *X-PLOR* (Brünger, 1992) were performed. In the final stages of refinement, individual temperature factors were also refined. Solvent molecules were included if they were on sites of difference electron density with values above 2.5σ and if they were within 3.5 Å of the protein or of a solvent molecule. The correctness of the final model, namely the CDR's, was checked using simulated-annealing omit maps (Hodel, Kim & Brünger, 1992).

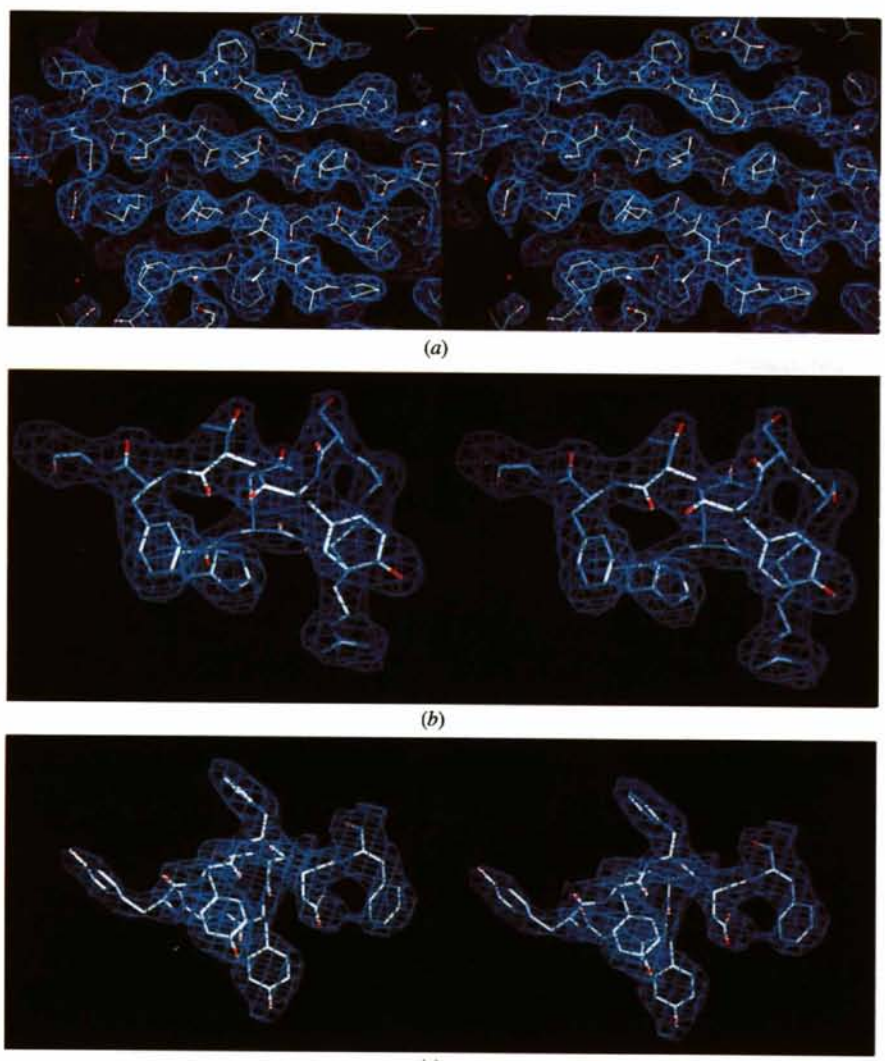

(*a*)

(*b*)

(*c*)

Fig. 1. Stereo pairs showing electron density for the central β-sheet of C_H1 (*a*), for the L3 (*b*) and H3 (*c*) loops. The $(2|F_{obs}| - |F_{cal}|)\exp(i\varphi_{cal})$ map contoured at 1σ was calculated at 2.6 Å resolution using the final refined coordinates.

Table 3. *Results of structure refinement*

No. of SDZ CHI621 atoms	3234
No. of solvent molecules	69
Average B value for V_L and C_L atoms (Å^2)	29.2
Average B value for V_H and C_H1 atoms (Å^2)	30.4
Average B value for the solvent molecules (Å^2)	45.5
Range of spacings (Å)	8.0–2.6
R value (all data) (%)	19.7
No. of reflections	13210
Weighted r.m.s.d. from ideality	
Bond length (Å)	0.014
Bond angle (°)	3.38

3. Results

3.1. *Quality of the structure*

A representative region of the electron-density map is shown in Fig. 1. The quality of the map is, in general, quite high and with the exception of one disordered region (in the constant domain, H_128–H_138), allowed confident placement of most main- and side-chain atoms. Because inclusion of the loop H_128–H_138 very slightly improves the R factor, it was kept during refinement, however the atomic coordinates of these residues are likely to be subject to error. The electron density for the vast majority of backbone carbonyl atoms was clearly visible providing confidence that the φ and ψ angles were essentially correct. A Ramachandran plot is given in Fig. 2. The only non-glycine residues with φ, ψ outside the allowed regions, (H_S130, $\varphi = 14°$, $\psi = 123°$) according to the *PROCHECK* program (Laskowski, MacArthur, Moss & Thornton, 1993), occurs in the disordered regions of the map. The structure of the SDZ CHI621 Fab has been refined to an R factor of 19.7% for 13210 unique reflections between 8 and 2.6 Å (all data up to this resolution range). The data of the crystallographic refinement are presented in Table 3. High-resolution data are weak and might account for the relatively high values of B factors in some part of the structure (Fig. 3). The highest B factors are in the solvent-exposed loop areas of the structure, namely in the H_128–H_138 loop, which shows very poor density as previously observed for others Fab structures whereas the lowest B factors are located in the β-sheets.

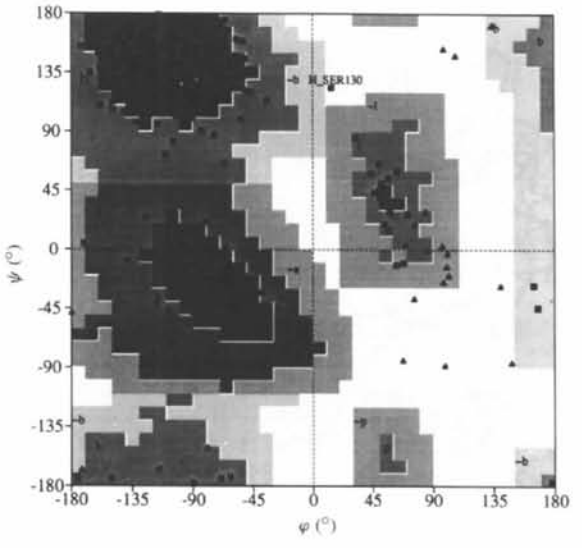

Fig. 2. Ramachandran plot (φ, ψ) for the SDZ CHI621 Fab fragment. According to the *PROCHECK* program (Laskowski *et al.*, 1993), the [*A,B,L*] areas correspond to the most favoured regions of the Ramachandran plot, [*a,b,l,p*] to the additional allowed regions and [~*a*, ~*b*, ~*l*, ~*p*] to the generously allowed regions, respectively. The triangles represent glycine residues. The only residue which lies in disallowed regions is H_SER130.

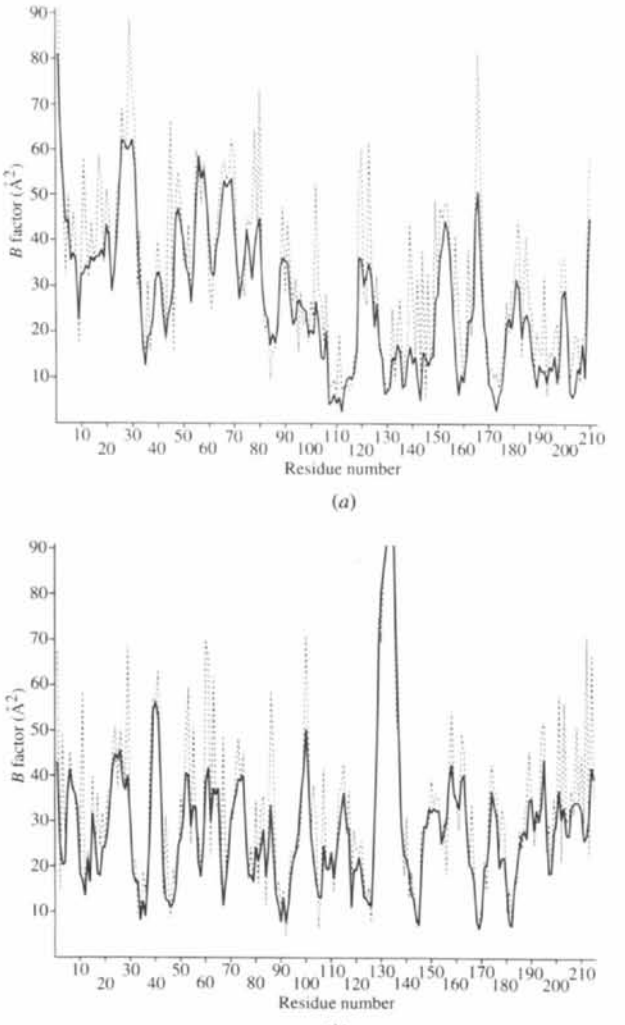

Fig. 3. Average main-chain (N, C$^\alpha$, C) (continuous lines) and side-chain (broken lines) temperature factors as a function of residue number for the light (*a*) and heavy (*b*) chains of the Fab fragment of SDZ CHI621.

Table 4. *Superposition of SDZ CHI621 Fab on other Fab C^{α} coordinates*

R.m.s. differences in atomic coordinates (Å) following superposition of the C^{α} backbone with other known Fab structures. The superposition was performed with the program *O* (Jones *et al.*, 1991). The coordinates for HyHel-5 (Sheriff *et al.*, 1987), D1:3 (Fishmann *et al.*, 1991), KOL (Marquart *et al.*, 1980), J539 (Suh *et al.*, 1986) were obtained from the Brookhaven Protein Data Bank. The V_L and V_H domains were superimposed with the hypervariable loops deleted. For the C_L domains and C_H1 domains, all residues were used. The V_L/V_H and C_L/C_H1 superpositions consisted of simultaneous superposition of the V_L and V_H domains and of the C_L and C_H1 domains, respectively.

Antibody	V_L	V_H	V_L/V_H	C_L	C_H1	C_L/C_H1
HyHel-5	0.47	0.64	0.81	0.92	2.73	2.01
D1:3	0.63	1.02	1.10	0.66	2.76	2.02
KOL	2.02	1.14	3.16	3.75	1.48	3.30
J539	0.50	0.95	1.12	0.70	3.47	2.54

3.2. *Overall structure*

The structure shows the typical Fab immunoglobulin fold, and backbone atoms can be readily superposed on other Fab structures (Table 4). The V_L and V_H domains of SDZ CHI621 are structurally most similar to the V_L and V_H domains of HyHel5 (Sheriff *et al.*, 1987). The result of the comparisons of SDZ CHI621 C_L domain shows a good match with those of HyHel5, D1:3 and of J539 presumably because their light chains are all κ chains (KOL has a λ-type light chain). Not surprisingly the C_H1 domain best matches with that of KOL which has a human $\gamma 1$ sequence. Fig. 4 compares the C^{α} traces of the 5DZ CHI621 Fab with that of HyHel5. The elbow angle, defined as the angle between the C_H1/C_L and V_H/V_L pseudo-dyad axes, is 162°.

3.3. *CDR analysis*

The analysis of the CDR's was performed according to the scheme of canonical loops structures developed by Chothia *et al.* (1989). It appears that L1, L2, H1 and H2* superimpose very well onto canonical CDR loops and could be readily compared with the CDR's of HyHel5 (Table 5) although some of their residues are involved in crystal-packing interactions. The CDR3 of the light chain is relatively short as it consists of only seven residues (H88-Q89-R90-S91-S92-Y93-T94). It does not fall into any of the reported classes and it might represent a novel type of L3 loop. Its conformation resembles more a slightly distorted type I β-turn between residues R90 and Y93. For type I β-turn, it was noticed that there often exists a hydrogen bond between the N—H(i+2) of the middle peptide and the side chain of residue i when it is either Asp, Asn or Ser (Wilmot & Thornton, 1988). This interaction makes these turns very stable. In the case of L3 the residue i is R90, hence its side chain is on one hand too long to form the hydrogen bond and on the other is not a good hydrogen-bond acceptor. Actually the side-chain atoms of R90 fold back towards the V_H domain. Interestingly residue $i-1$ (Q89) with its side-chain atoms provides the stabilizing hydrogen-bond acceptor

* L1 is the light chain of CDR1, L2 is the light chain of CDR2, L3 is the light chain of CDR3, H1 is the heavy chain of CDR1, H2 is the heavy chain of CDR2 and H3 is the heavy chain of CDR3.

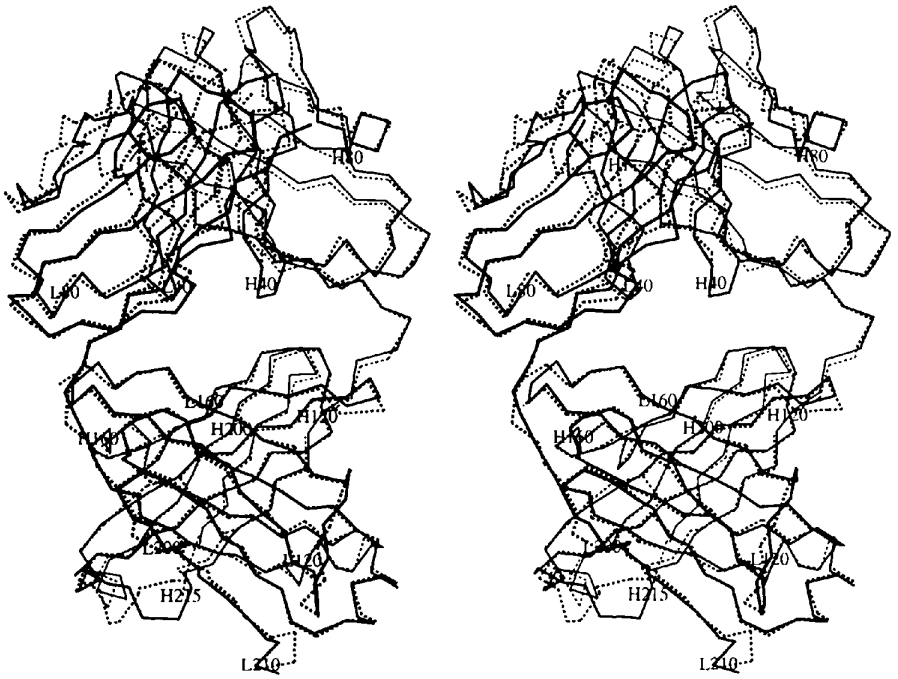

Fig. 4. Comparison of the Fab fragment of SDZ CHI621 with that of HyHel-5. Stereoviews of the superposition of the C^{α} atoms trace of SDZ CHI621 (plain lines) on that of HyHel5 (dotted lines) (Sheriff *et al.*, 1987). Every 40th C^{α} of SDZ CHI621 is labelled. The pictures representing molecules were prepared with the program *MOLSCRIPT* (Kraulis, 1991).

Table 5. *Results of superposition of CDR's with backbone atoms (N, C^{α}, C, O)*

The comparisons were made with the coordinates of HyHel-5 (Sheriff *et al.*, 1987) as it appears that SDZ CHI621 and HyHel-5 loops belong to the same categories except for L3 which could not be classified.

Loop	Type	R.m.s.d. (Å)
L1	1	1.1
L2	1	0.95
L3	None	—
H1	1	0.68
H2	2	1.06

Table 6. *Intramolecular and intermolecular hydrogen bonds between the L3 and H3 loops*

Protein atoms	Distance	Protein atoms
Intramolecular hydrogen bonds	(Å)	
L-His88 $N^{\varepsilon 2}$	3.2	L_Tyr93 O
L_Gln89 $O^{\varepsilon 1}$	2.9	L_Ser91 N
L_Ser92 O	3.1	L_Thr94 N
H_Asp97 $O^{\varepsilon 1}$	3.1	H_Gly99 N
H_Tyr98 N	3.0	H_Tyr101 O
Intermolecular hydrogen bonds		
L_Arg90 $N^{\eta 1}$	2.8	H_Asp97 $O^{\varepsilon 1}$
L_Arg90 $N^{\eta 1}$	2.8	H_Asp97 $O^{\varepsilon 2}$
L_Arg90 $N^{\eta 1}$	2.6	H_Gly99 O
L_Arg90 $N^{\eta 2}$	2.7	H_Asp97 $O^{\varepsilon 1}$

atom as the O^{ε} atom lies within 2.9 Å of the N—H of residue $i+2$. This interaction certainly stabilizes the conformation of the L3 loop as does the hydrogen bond between the $N^{\varepsilon 2}$ of H88 and the carbonyl O atom of Y93. Four residues (H88, R90, S91 and S92) out of the seven of this loop are involved with their side-chain atoms in hydrogen-bond interactions either with the V_L or V_H domains further limiting the flexibility of the loop. The L3 loop can be regarded as relatively rigid as typified by an average *B* factor of 32.2 Å. This latter value is comparable to the value observed for the light-chain atoms (29.2 $Å^2$). The conformation of the L3 loop is presumably influenced as well by the existence of a salt bridge between the guanidinium group of R90 from L3 and the carboxylate group of D97 from H3 (see below) (Fig. 5, Table 6).

The H3 loop is composed of eight amino-acid residues (D97-Y98-G99-Y100-Y101-F102-D1030-F104) and its length is characteristic of mouse H3 loop (Wu, Johnson & Kabat, 1993). It lies in well defined electron density and has an average *B* factor of 37.2 $Å^2$ (Fig. 1). Its conformation is stabilized by an intramolecular

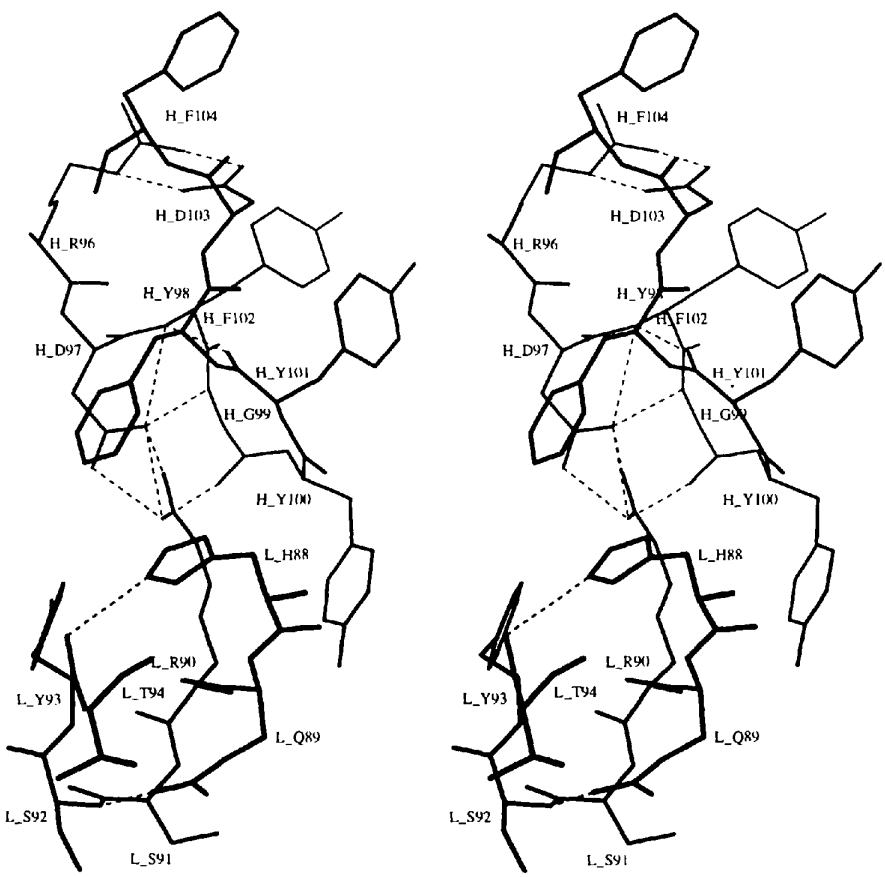

Fig. 5. Intermolecular interactions between the L3 and H3 loops of SDZ CHI621. The L3 and H3 loop residues and their labels are shown with black plain lines. Hydrogen bonds are represented as dashed lines and the values of the corresponding distances are given in Table 6.

hydrogen bond between the amide N atom of Y98 and the carbonyl O atom of Y101. The O^{δ} atoms of the two aspartate residues form favorable interactions with the following amide as commonly observed. There is a network of interaction between the L3 and H3 loops which seems dominated by the salt bridge between L_R90 and H_D97 whereby the carbonyl O atom of H_Y98 is also engaged in a hydrogen-bond interaction with the guanidinium group of L_R90 (Fig. 5). This contact is further strengthened by hydrophobic aromatic interactions as the $C^{\varepsilon 1}$ atom of L_H88 lies within 3.3 Å of H_F102. The existence of these contacts probably induces the bending of L3 towards the H3 loop and is likely to couple together the movement of those two loops. Contacts between H3 and L3 loops in antibody structures are commonly observed but they are usually dominated by hydrophobic interactions. Neither the L3 loop nor the H3 loop are involved in crystal-packing interactions.

A total of 53 residues are associated with the CDR's and together they represent a solvent-accessible surface area of 2828 $Å^2$ which accounts for 14.9% of the total accessible surface area. Interestingly the two CDR3 loops, which are usually mostly involved in antigen recognition, show a lower average accessible surface area per residue (L3:25 $Å^2$; H3:45 $Å^2$) than the four other CDR's (average of 60 $Å^2$). These small values observed for L3 and H3 are likely a result of the small size of L3 and of their intermolecular interactions (Fig. 5). However one cannot rule out that the salt bridge between L3 and H3 is broken down during antigen recognition thus leaving L3 and H3 free for binding. It was noticed that certain amino acids (Tyr, Ser, Asn, Trp) are more likely to be found in the

Table 7. *Intermolecular hydrogen bonds between V_L and C_L*

V_L atoms	Distance (Å)		Distance (Å)	C_L atoms
Ser12 O^{γ}	2.9	W8	3.1	Tyr170 O^{η}
Glu102 $O^{\varepsilon 2}$	2.8	W8	3.1	Tyr170 O^{η}
Lys100 N^{ζ}			2.9	Glu162 $O^{\varepsilon 1}$
Lys100 N^{ζ}			3.0	Glu162 $O^{\varepsilon 2}$
Glu102 $O^{\varepsilon 1}$			3.2	Tyr170 O^{η}
Glu102 $O^{\varepsilon 2}$			2.9	Tyr170 O^{η}
Ile103 N			3.2	Gln163 $O^{\varepsilon 1}$
Ile103 O			2.9	Gln163 $N^{\varepsilon 2}$
Arg105 N^{ε}			3.1	Asp167 O
Arg105 $N^{\eta 2}$			3.3	Asp167 O

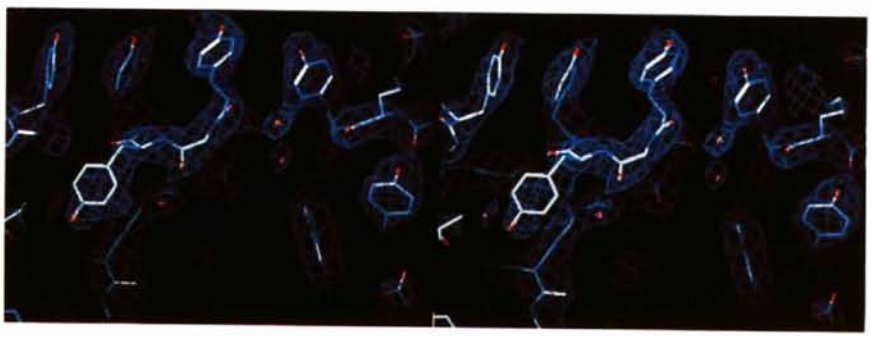

Fig. 6. Stereo pairs showing electron density for the array of aromatic residues within the CDR's. From left to right, it comprises L_Y48, H_Y101, H_Y100, H_Y98, H_Y30, H_Y50, H_W31. The $(2|F_{obs}| - |F_{cal}|)\exp(i\varphi_{cal})$ map contoured at 1σ was calculated at 2.6 Å resolution using the final refined coordinates.

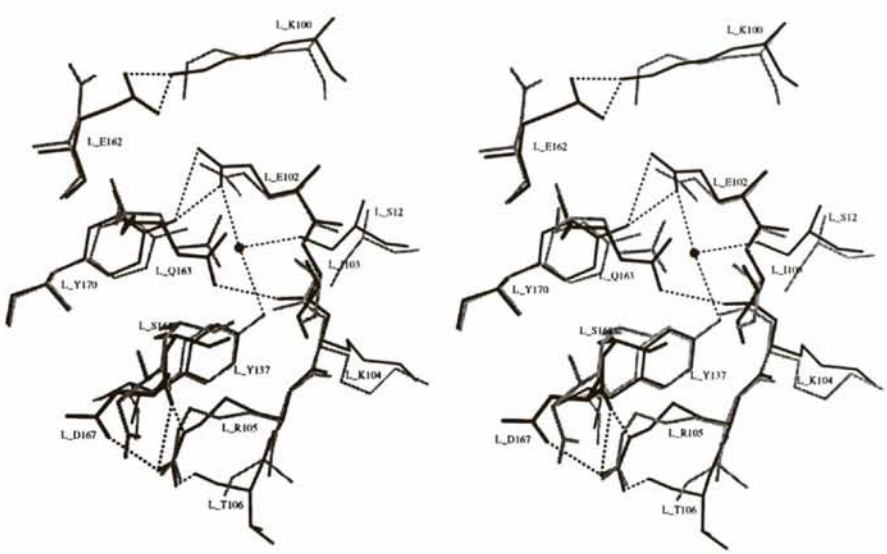

Fig. 7. Effect of the chimerization. Comparison of the intermolecular interactions between V_L and C_L for SDZ and CHI621 and for HyHel-5 (distance cutoff 3.5 Å). The 11 residues of the light chain of SDZ CHI621 (K100, E102, I103, L104, R105, T106, Y137, E162, Q163, S168, Y170) are represented with black plain lines and the corresponding residues in HyHel-5 with gray plain lines. Within this set of residues, there are only two differences in sequence between both antibodies: T106 and E162 are substituted by A106 and D162, respectively, in HyHel-5. The solvent molecule (W8) is shown as a black-filled circle and hydrogen bonds with dashed lines. Values of the hydrogen bonds distances are given in Table 7.

antigen-combining sites (Lea & Stuart, 1995). There are eight tyrosines, 11 serines, two asparagines and one tryptophan in the CDR's of SDZ CHI621 out of 53 residues. One striking feature of the antigen combining site is the presence of one tryptophan and six tyrosines lined up in a linear fashion within 21 Å (Fig. 6). Five of these are pointed out towards the same direction into the solvent and it is likely that the sixth one could flip up its side chain to point into the same direction upon antigen binding providing an array of aromatic residues for interaction.

3.4. *Chimerization*

In cross-inhibition studies, SDZ CHI621 and RFT5, the murine CD25 mAb from which it is derived, show identical receptor blocking profiles indicating that the genetic recombination had not affected binding specificity, affinity or avidity (Amlot *et al.*, 1995). A comparison of the conformation of the 11 residues of SDZ CHI621 which are involved in the contacts between V_L and C_L with those of HyHel-5 show that they adopt identical conformation as typified by an r.m.s.d. of 0.25 Å for all atoms (Fig. 7). There are two differences in sequence between both antibodies: T106 and E137 are substituted for by Ala and Asp in HyHel-5, respectively. The change Ala/Thr does not seem to affect the pattern of interaction between V_L and C_L whereas the association between V_L and C_L (Table 7) has been strengthened by the presence of E137 (instead of Asp for HyHel-5). Because Glu contains an extra C atom in its side chain, it can make a salt-bridge interaction with K100. In HyHel-5 there is only one hydrogen-bond interaction between V_H and C_H1, whereby the O^{γ} of S115 lies within 2.9 Å from the $O^{\delta 1}$ of D176. In the sequence of SDZ CHI621 this aspartate is replaced by a glycine residue and cannot therefore make any hydrogen-bond interactions. The fact that no electrostatic interactions maintain the association between V_H and C_H1 presumably contributes to the slightly more extended conformation of SDZ CHI621 (elbow angle of 162°) when compared with HyHel (155°).

In summary, this structure is to our knowledge the second structure of a Fab fragment from a chimeric antibody (Brady *et al.*, 1992). It shows that the conformation of the Fab fragment of SDZ CHI621 looks very similar to the one commonly observed for murine Fab's which is of great importance for clinicians in the view of its therapeutic use. The next step to 'human' antibodies would be to transplant CDR's from SDZ CHI621 onto a human framework. CDR-grafted antibodies, which are more than 90% human, are likely to be less immunogenic than their chimeric counterparts which have C_H1 and C_L human and the rest (V_H and V_L) being murine. The crystal structure of SDZ CHI621 could provide a good starting base to perform humanization in an optimized way. However, in the clinical studies carried out (Amlot *et al.*, 1995), no antibody response was detected in any of the patients treated with SDZ CHI621, suggesting that humanization is unlikely to be necessary for the development of a successful mAb drug.

Atomic coordinates and structure factors have been deposited with the Protein Data Bank.*

The author thanks H.P. Kocher's team for providing the antibody, M. H. Schreier for critically reading the manuscript, and J. Kallen and M. D. Walkinshaw for constant support.

* Atomic coordinates and structure factors have been deposited with the Protein Data Bank, Brookhaven National Laboratory (Reference: 1MIM, R1MIMSF). Free copies may be obtained through The Managing Editor, International Union of Crystallography, 5 Abbey Square, Chester CH1 2HU, England (Reference: AD0014). At the request of the authors, the atomic coordinates will remain privileged until 1 May 1997 and the structure factors will remain privileged until 1 May 2000.

References

Amlot, P. L., Rawlings, E., Fernando, O. N., Griffin, P. J., Heinrich, G., Schreier, M. H., Castaigne, J.-P., Moore, R. & Sweny, P. (1995). *Transplantation*, **60**, 748–756.

Brady, R. L., Edwards, D. J., Hubbard, R. E., Jiang, J.-S., Lange, G., Roberts, S. M., Todd, R. J., Adair, J. R., Emtage, J. S., King, D. J. & Low, D. C. (1992). *J. Mol. Biol.* **227**, 253–264.

Brünger, A. T. (1992). *X-PLOR Version 3.1 Manual.* Howard Hughes Medical Institute and Department of Molecular Biophysics and Biochemistry, Yale University, New Haven, CT, USA

Chothia, C., Lesk, A. M., Tramontano, A., Levitt, M., Smith-Gill, S. J., Air, G., Sheriff, S., Padlan, E. A., Davies, D., Tulip, W. R., Colman, P. M., Spinelli, S., Alzari, P. M. & Poljak, R. J. (1989). *Nature (London)*, **342**, 877–883.

Collaborative Computational Project, Number 4. (1994). *Acta Cryst.* D**50**, 760–763.

Fishmann, T. O., Bentley, G. A., Bhat, T. N., Boulot, G., Mariuzza, R. A., Phillips, S. E. V., Tello, D. & Poljak, R. J. (1991). *J. Biol. Chem.* **266**, 12915–12920.

Hodel, A., Kim, S.-H. & Brünger, A. T. (1992). *Acta Cryst.* A**48**, 851–858.

Jones, A. T., Zou, J.-Y., Cowan, S. W. & Kjeldgaard, M. (1991). *Acta Cryst.* A**47**, 110–119.

Kabat, E. A., Wu, T. T., Reid-Miller, M., Perry, H. M., Gottesman, K. S. & Foeller, C. (1991). *Sequences of Proteins of Immunological Interest,* 5th ed., Bethesda, MD. National Institutes of Health.

Kraulis, P. J. (1991). *J. Appl. Cryst.* **24**, 946–950.

Kupiec-Weglinski, J. W. Diamantstein, T. & Tilney, N. L. (1988). *Transplantation*, **46**, 785–787.

Laskowski, R. A., MacArthur, M. W., Moss, D. S. & Thornton, J. M. (1993). *J. Appl. Cryst.* **26**, 283–291.

Lea, S. & Stuart, D. (1995). *FASEB J.* **9**, 87–93.

Marquart, M., Deisenhofer, J., Huber, R. & Palm, W. (1980). *J. Mol. Biol.* **141**, 369–391.

Messerschmidt, A. & Pflugrath, J. W. (1987). *J. Appl. Cryst.* **20**, 306–315.

Sheriff, S., Silverton, E. W., Padlan, E. A., Cohen, G. H., Smith-Gill, S. J., Finzel, B. & Davies, D. R. (1987). *Proc. Natl Acad. Sci. USA,* **84**, 8075–8079.

Suh, S. W., Bhat, T. N., Navia, M. N., Cohen, G. H., Rao, D. N., Rudikoff, S. & Davies, D. R. (1986). *Proteins Struct. Funct. Genet.* **1**, 74–80.

Tilney, N. L., Milford, E. L., Aravjo, J.-L., Strom, T. B., Carpenter, C. B. & Kirkman, R. L. (1984). *Ann. Surg.* **200**, 605–613.

Wilmot, C. M. & Thornton, J. M. (1988). *J. Mol. Biol.* **203**, 221–232.

Wu, T. T., Johnson, G. & Kabat, E. A. (1993). *Proteins,* **16**, 1–7.